

Why did you predict that? Towards explainable artificial neural networks for travel demand analysis

Alwosheel, Ahmad; van Cranenburgh, Sander; Chorus, Caspar G.

DOI

[10.1016/j.trc.2021.103143](https://doi.org/10.1016/j.trc.2021.103143)

Publication date

2021

Document Version

Final published version

Published in

Transportation Research Part C: Emerging Technologies

Citation (APA)

Alwosheel, A., van Cranenburgh, S., & Chorus, C. G. (2021). Why did you predict that? Towards explainable artificial neural networks for travel demand analysis. *Transportation Research Part C: Emerging Technologies*, 128, Article 103143. <https://doi.org/10.1016/j.trc.2021.103143>

Important note

To cite this publication, please use the final published version (if applicable). Please check the document version above.

Copyright

Other than for strictly personal use, it is not permitted to download, forward or distribute the text or part of it, without the consent of the author(s) and/or copyright holder(s), unless the work is under an open content license such as Creative Commons.

Takedown policy

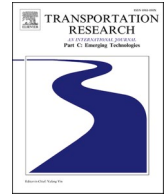
Please contact us and provide details if you believe this document breaches copyrights. We will remove access to the work immediately and investigate your claim.



ELSEVIER

Contents lists available at [ScienceDirect](https://www.sciencedirect.com)

Transportation Research Part C

journal homepage: www.elsevier.com/locate/trc

Why did you predict that? Towards explainable artificial neural networks for travel demand analysis

Ahmad Alwosheel^{a,b,*}, Sander van Cranenburgh^b, Caspar G. Chorus^b

^a King Abdulaziz City for Science and Technology, Saudi Arabia

^b Transport and Logistics Group, Department of Engineering Systems and Services, Delft University of Technology, the Netherlands

ARTICLE INFO

Keywords:

Travel choice analysis
Explainability
Black-box issue
Artificial Neural Networks

ABSTRACT

Artificial Neural Networks (ANNs) are rapidly gaining popularity in transportation research in general and travel demand analysis in particular. While ANNs typically outperform conventional methods in terms of predictive performance, they suffer from limited explainability. That is, it is very difficult to assess whether or not particular predictions made by an ANN are based on intuitively reasonable relationships embedded in the model. As a result, it is difficult for analysts to gain trust in ANNs. In this paper, we show that often-used approaches using perturbation (sensitivity analysis) are ill-suited for gaining an understanding of the inner workings of ANNs. Subsequently, and this is the main contribution of this paper, we introduce to the domain of transportation an alternative method, inspired by recent progress in the field of computer vision. This method is based on a re-conceptualisation of the idea of ‘heat maps’ to explain the predictions of a trained ANN. To create a heat map, a prediction of an ANN is propagated backward in the ANN towards the input variables, using a technique called Layer-wise Relevance Propagation (LRP). The resulting heat map shows the contribution of each input value –for example the travel time of a certain mode– to a given travel mode choice prediction. By doing this, the LRP-based heat map reveals the rationale behind the prediction in a way that is understandable to human analysts. If the rationale makes sense to the analyst, the trust in the prediction, and, by extension, in the trained ANN as a whole, will increase. If the rationale does not make sense, the analyst may choose to adapt or re-train the ANN or decide not to use it at all. We show that by reconceptualising the LRP methodology towards the choice modelling and travel demand analysis contexts, it can be put to effective use in application domains well beyond the field of computer vision, for which it was originally developed.

1. Introduction

Artificial Neural Networks (ANNs) are emerging as an increasingly indispensable tool for many applications in the field of transportation. Recent examples include modelling lane-changing behaviour of drivers (Xie, Fang, Jia, & He, 2019), predicting mode choice behaviour (Sun et al., 2018), predicting traffic flow (Polson & Sokolov, 2017), uncovering the value-of-travel-time distribution (Van Cranenburgh & Kouwenhoven, 2020; Van Cranenburgh et al., 2021). This increase in ANNs’ popularity in transportation research is mainly driven by the recent abundance of data stemming from a variety of emerging sources (Chen, Ma, Susilo, Liu, &

* Corresponding author.

E-mail address: aalowsheel@kacst.edu.sa (A. Alwosheel).

<https://doi.org/10.1016/j.trc.2021.103143>

Received 23 January 2020; Received in revised form 16 February 2021; Accepted 8 April 2021

Available online 19 May 2021

0968-090X/© 2021 The Authors. Published by Elsevier Ltd. This is an open access article under the CC BY license

(<http://creativecommons.org/licenses/by/4.0/>).

Nomenclature

V_i	Observed part of utility of alternative i
ASC_i	Specific constant of alternative i
β_{TT}	Taste parameter associated with travel time attribute
β_{TC}	Taste parameter associated with travel cost attribute
β_{AG_TC}	Taste parameter associated with interaction between age and travel cost attribute
β_{DIS_TC}	Taste parameter associated with interaction between travel distance and travel cost attribute
β_{FEM_TC}	Taste parameter associated with interaction between gender and travel cost attribute
β_{DL}	Taste parameter associated with driving license attribute
β_{CO}	Taste parameter associated with number of owned car attribute
β_{TRAF}	Taste parameter associated with traffic variability attribute
β_{INTER}	Taste parameter associated with number of interchanges attribute

Wang, 2016), and the ANN's often impressive predictive performance (Goodfellow, Bengio, & Courville, 2016; Karlaftis & Vlahogianni, 2011; Mckinney et al., 2020).

Although ANNs often obtain superior prediction performance compared to their conventional, more theory-driven statistical or econometric counterparts (e.g. discrete choice models in a travel demand analysis context), their opaque nature makes it very difficult to explain individual predictions which are made by an ANN. Without sufficient understanding of how and why the trained ANN makes a particular prediction, the use of ANNs in transportation research will mainly be confined to niche settings where prediction performance is highly valued (e.g., short term travel demand predictions) and model transparency is not of great importance; for justifiable reasons, governments and transport planning agencies put a higher premium on model transparency (which is considered a prerequisite for good governance), than on superior empirical prediction performance.

Recently, the development of techniques for opening up and explaining the ANN's black-box has been the subject of many research efforts in a variety of research fields (Lipton, 2016). Notably, in the computer vision field much progress has been made to shed light on the inner workings of trained ANNs (Montavon, Samek, & Müller, 2018; Samek, Wiegand, & Müller, 2017; Simonyan, Vedaldi, & Zisserman, 2013). The Layer-wise Relevance Propagation (LRP) method has emerged as one of the most popular approaches to inspect the rationale behind ANNs' predictions (Adebayo et al., 2018). The LRP method is a post-hoc approach (i.e., applied after having trained the ANN) which is used to explain a specific prediction of the trained ANN by generating a so called heat map. More specifically, the LRP method uses the topology of the ANN to assign a relevance score to each independent variable, highlighting the most relevant independent variables in the context of a particular prediction. These resulted relevance scores are then used to generate a heat map. For example, the heat map of an ANN trained to discriminate between dogs and cats based on pictures, highlights which parts of an image (e.g., pixels representing cat whiskers) were most relevant for the produced prediction (in casu: cat). The generated heat map reveals the rationale of a trained ANN and as such allows for intuitive investigation of what made the model produce a prediction; in case the rationale aligns with the mental map of the analyst, this helps to build trust in that prediction. In case the exhibited rationale does not align, this of course still offers valuable information to the analyst. In principle, LRP (and related techniques) could be of use to analysts working in other contexts than computer vision, including transportation. But, to the best of the authors' knowledge, no studies have yet investigated the use of LRP-based heat maps for transportation research in general and travel demand analysis in specific; this is possibly due to the fact that the analogy between picture classification (the original domain of LRP) and travel demand predictions is not directly obvious.

This paper re-conceptualises the use of LRP-based heat map generation and pioneers its use in a transportation (travel demand analysis) context.¹ In particular, we show that by properly reconceptualising the notion of LRP-based heat maps using Monte-Carlo experiments, they can provide meaningful explanations for predictions made by ANNs which were trained for predicting travel mode choices.² As such, our paper presents a method to help analysts gain trust in ANNs' predictions in travel behaviour contexts (as well as in choice modelling contexts more generally). Furthermore, we show that by carefully selecting which predictions to analyse, the process of heat map generation can be used to build trust in the trained ANN as a whole (as opposed to be used to explain individual predictions made by an ANN). For the empirical part of our study, we use a recently collected Revealed Preference (RP) mode choice data dataset (Hillel, Elshafie, & Ying, 2018). For future researchers to replicate our work, the codes and datasets used in this paper can be found in a GitHub repository: <https://github.com/The-Ahmad/explainable-anns-for-travel-demand-analysis>.

Before we proceed, we would like to emphasise once more that this research is motivated by the observation that ANNs are increasingly used for travel demand analysis and prediction. This in our view presents a strong motivation to offer a method which reveals the rationale behind a trained ANN and as such allows for intuitive investigation of what made the model produce a prediction.

¹ Note that heat mapping (as a technique to facilitate interpretation of the outcomes of the LRP method) has been widely used particularly in the context of image processing and computer vision. In the context of transportation, the technique has been also adopted for this purpose (see (Ma et al., 2017) and (Yao et al., 2018) for recent examples), but not before to model travel choices.

² Note that the re-conceptualisation effort includes investigation of how the LRP-based heat map results can be interpreted, a part that is highly important particularly in the context of discrete choice analysis.

Table 1
Basic image processing terminology and discrete choice modelling equivalent.

Image processing	Discrete choice modelling
Pixel	Attribute
Intensity	Value
Label/Class	Alternative
Label set	Choice set

This research does explicitly not aim to compare the pros and cons of ANNs and traditional discrete choice models in order to make normative judgements about which modelling paradigm is better.

The remainder of this paper is organised as follows: [Section 2](#) introduces the used methodology and establishes the analogy between travel mode choice modelling and image classification. [Section 3](#) presents the dataset used for our analysis and discusses the ANN training procedure. [Section 4](#) presents the results. It shows the heat maps created using LRP. [Section 5](#) draws conclusions and shows directions for future research.

2. Methodology

Before delving into the LRP methodology details, we present notations and establish the analogy between image classification and discrete (travel mode) choice modelling. Numerous concepts in discrete choice modelling have a counterpart, under a different name, in machine learning. For the reader's convenience [Table 1](#) provides a brief 'translation' table.

In discrete choice analysis the choice data consists of a set of observations $S = ((\mathbf{x}_1, y_1), (\mathbf{x}_2, y_2), \dots, (\mathbf{x}_n, y_n), \dots, (\mathbf{x}_N, y_N))$. Each n^{th} observation s_n contains a vector of independent variables \mathbf{x}_n that represent the attributes and a K -dimensional vector of dependent variables y_n that represents the observed choice (i.e., zeros for the non-chosen alternatives, and one for the chosen alternative); K being the size of the choice set. Each vector \mathbf{x}_n consists of I independent variables (annotated as x_i). Since choices are mutually exclusive (i.e., only one alternative can be chosen from the choice set), from a machine learning perspective this is considered a classification problem.

In image classification problems each observation contains an array of pixels of the image and a Q -dimensional vector that represents the image label; Q being the size of the fixed set of categories. For simplicity we consider the case of a greyscale image where each pixel takes a single value that represents intensity within some range (e.g., from 0 (black) to 255 (white)).³ The task of image classification is to assign an input data to one label from the fixed set of categories. In this setting, an analogy between image classification and discrete choice modelling can be drawn, where pixels are equivalent to attributes (e.g. travel time), and intensity corresponds to the attribute value (e.g. 25 min). Further, similar to the observed choice set, the image label set of size Q is finite, collectively exhaustive and mutually exclusive.

When using ANNs for classification, the so-called softmax function is used at the output layer to convert values (processed and forwarded by hidden layers) into probabilities. The softmax is essentially a logit function, see [Appendix A](#) for a brief description of the ANN methodology. Similar to discrete choice models, ANNs make predictions up to a probability. Since this study is primarily concerned with explaining predictions of ANNs by uncovering the relevance of each independent variable to a particular prediction, the values processed and forwarded to the output layer (i.e., softmax function inputs) are annotated $f(x)$ and are henceforth referred to as the *relevance*. Note that the notion of relevance in this context can loosely be conceived as utilities in a discrete choice context.

2.1. Model explainability and trust

Opening or greying the black-box of ANNs has received much attention in a variety of fields ([Alwosheel et al., 2019](#); [Hall and Gill, 2018](#)). In the literature, several meanings have been attached to this effort such as enhancing interpretability, explainability and understandability ([Doshi-Velez & Kim, 2017](#); [Lipton, 2016](#); [Rosenfeld & Richardson, 2019](#)). In this study, we focus on explainability, which is defined as the ability of the analyst to inspect the contribution of each input (in the computer vision case, pixels of a picture; in our travel demand analysis case, attribute values of travel choice alternatives or characteristics of the decision maker) to produce a prediction ([Montavon et al., 2018](#)). By explaining a model prediction, we mean presenting a numerical or visual artefact that provides a qualitative understanding of the relationship between independent variables (in our case, attributes) and the model's prediction ([Ribeiro, Singh, & Guestrin, 2016](#)). We consider the ability to explain predictions to be critical to build trust between the analyst and the trained ANN model (see further below). Moreover, in contrast to ante-hoc explainability where the focus is on incorporating explainability directly into the model structure (i.e., designing a model such that its predictions can be explained by the analyst), the focus of this paper is on post-hoc explainability (which comes after having trained a model, without elucidating or enforcing how the model works in terms of its structure).

For an analyst to trust a model prediction and take some actions (e.g. choose a policy or plan) based on it, it is essential to: 1) understand *why* the model has made this prediction (i.e., prediction explainability, henceforth called the Why part); 2) ensure that this

³ In other image types (e.g., RGB type), each pixels consist of several channels (e.g., red, green and blue channels).



Fig. 1. Rooster image (Samek et al., 2017). (For interpretation of the references to colour in this figure legend, the reader is referred to the online version of this article.)

rationale is based on ‘correct’, i.e. intuitive and expected relations (this is called the Domain Knowledge part). Obviously, the latter is domain dependent, and the analyst has the “final say” in this regard. For example, consider a black-box model trained to detect tumours from x-ray images. For a doctor to trust a model’s prediction, (s)he needs to understand on what basis or factors (e.g., which part of the x-ray) the model made that prediction (the Why part), and whether these are correct, intuitive and expected (based on the doctor’s Domain Knowledge). In the remaining part of Section 2, we focus on the Why part (i.e., we present an approach that enables an analyst to answer the Why question). The Domain Knowledge part will be elaborated as part of our discussion of the results of our empirical analysis in Section 4.

To address the Why part, so-called saliency methods have emerged as a popular tool to highlight which independent variables deemed relevant or important for an ANN prediction (Adebayo et al., 2018; Kittley-Davies et al., 2019; Simonyan et al., 2013). These methods can be broadly classified into two categories: perturbation- and backpropagation-based methods (Shrikumar, Greenside, & Kundaje, 2017).

Perturbation-based methods aim to measure the effect of applying small changes in each input (or removing it) on the predictions (or probabilities) produced by the trained ANN (Zeiler & Fergus, 2013; Zintgraf, Cohen, Adel, & Welling, 2017). The underlying principle of perturbation-based methods is that the input whose change or removal affects the ANN output most is the one that has the most relative importance (Ancona, Ceolini, Öztireli, & Gross, 2017). In applications of ANNs for travel choice behaviour modelling, most efforts to answer the Why part have indeed been devoted to perturbation-based approaches; this may be explained by their close analogy with the notion of elasticity, which is well-known in the travel behaviour research community (and in the choice modelling community more generally). For example, several studies conducted (or suggested using) perturbation-based methods – mostly called sensitivity analysis by transportation researchers – to measure the importance of independent variables for different types of trained ANNs (Chiang, Zhang, & Zhou, 2006; Golshani, Shabanpour, Mahmoudifard, Derrible, & Mohammadian, 2018; Hagenauer & Helbich, 2017; Hensher & Ton, 2000; Lee, Derrible, & Pereira, 2018).

While the perturbation-based methods are widely used to answer the Why part, several studies have highlighted their drawbacks and explained why they are fundamentally inappropriate for this aim. The first, more practical, drawback is that these methods can be computationally inefficient as each change (perturbation) requires a separate forward propagation for the ANN (Shrikumar et al., 2017). This aspect of computational (in-)efficiency becomes more important as the complexity and number of parameters of ANNs grow (e.g., an early version of a convolution neural network consists of over 60 million parameters (Krizhevsky, Sutskever, & Hinton, 2012)). The second, and more fundamental, drawback of perturbation-based methods is that upon close inspection, they do not actually provide an answer to the Why-question that analysts are looking for. Instead, because the process is based on alternation of independent variables’ values, perturbation based methods answer a different question, being *which* independent variable needs to be altered to make the example belong more, or less so, to the predicted alternative class. In other words, perturbation-based methods measure the susceptibility of the output to changes in the input, which might not necessarily coincide with insight into what are the inputs on which the network based its prediction (Böhle, Eitel, Weygandt, & Ritter, 2019; Montavon et al., 2018; Shrikumar et al., 2017). This is indeed a fundamental limitation when answering the Why question. A visual illustration of this subtle but fundamental point is presented by Samek et al. (2017) where an image of rooster is correctly predicted by the model (see Fig. 1). Changing the pixels’ values of the yellow flowers (that block part of the rooster) in a specific way would reconstruct the covered part of the rooster, which may result in an increase in the probability of predicting a rooster. As such, the result of this particular perturbation may lead the analyst to believe that pixels that constructed the yellow flowers were important to the prediction of rooster (which is certainly not correct).

In contrast to perturbation methods, backpropagation-based methods operate by propagating the relevance (i.e., softmax function input $f(x)$) from the output neuron backward through the hidden layers towards the input layer (see Appendix A for an overview of ANN structure) (Springenberg, Dosovitskiy, Brox, & Riedmiller, 2014). One of the most popular of this type of methods in the computer vision field is Layer-wise Relevance Propagation LRP (Bach et al., 2015). The LRP method leverages the structure of ANNs and the estimated model parameters (i.e., weights) to determine the negative/positive contribution of each independent variable to a

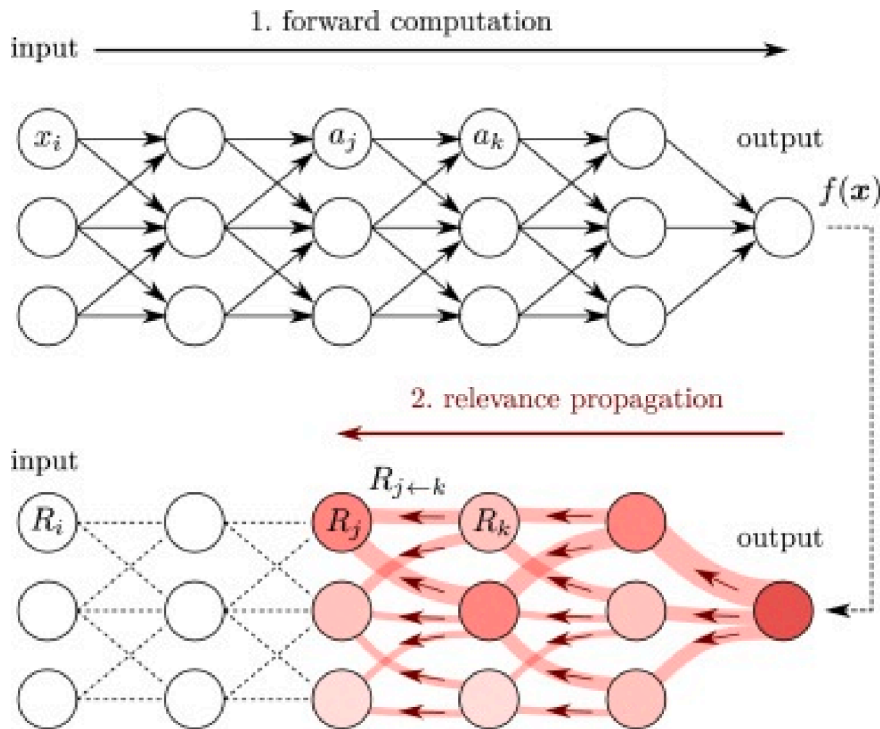


Fig. 2. Diagram of the LRP procedure (Montavon et al., 2018). Red arrows indicate the relevance propagation flow. (For interpretation of the references to colour in this figure legend, the reader is referred to the Web version of this article.) (<http://www.heatmapping.org/>)

particular prediction. It basically asks, for each node, which of the nodes in the preceding layer contributed, and to what extent, to the value in that node. As such, after being applied to the full network, it identifies the independent variables that were pivotal for the ANN's prediction. Thereby, LRP allows the analyst to understand *why* the model has made a particular prediction, given a set of independent variables (Samek, Montavon, Vedaldi, Hansen, & Müller, 2019). Furthermore, as these methods require a single pass to propagate the relevance from the output to the input layer, they are computationally highly efficient (Böhle et al., 2019). Colloquially put in the context of (travel) choice analysis, in contrast to perturbation methods which in essence inspect choice probabilities for other than a particular observation (by changing the input variables and looking at changes in choice probabilities), the LRP method only focuses on the particular observation to be explained, studying which input values were particularly crucial for the ANN to arrive at a prediction in the context of the observation.

Before we delve into the technical details, we would like to make a clear distinction between two types of trust: 1) trusting a particular prediction made by an ANN; and 2) trusting the ANN model as a whole. In its core, the LRP method is developed for the former type, but it is worth noting that the method can be also used for the latter type of trust by applying the method to many carefully selected observations (Ribeiro et al., 2016). In this study, we show how to use the method to gain trust in multiple ANN predictions (to build trust in each of those predictions). Then, we show a case of how trusting multiple systematically selected ANN predictions can lead to increased levels of trust in the model as a whole (see Section 4).

2.2. Layer-wise relevance propagation method

LRP is a post-hoc method proposed as a solution to explain what independent variables are relevant for reaching a specific prediction. The method has been originally developed in the context of computer vision Bach et al. (2015) and has been used across a range of disciplines (e.g., health care (Böhle et al., 2019; Sturm, Lapuschkin, Samek, & Müller, 2016)). In terms of explainability, it has been shown to be superior to alternative methods (e.g., perturbation based methods) in multiple natural imaging data sets (Samek, Binder, Montavon, Lapuschkin, & Müller, 2016).

LRP operates by propagating the activation strength of the node of interest backward, through hidden layers, to the input layer. In this study, we limit our focus on understanding the ANN prediction; hence, we are mainly concerned with back propagating the activation at the *output* nodes backwards through the hidden layers, using local propagation rules, until a relevance score R_i is allocated to each *input* variable x_i (Samek et al., 2017). Each R_i can be interpreted as the contribution an input x_i has made to a prediction (see Fig. 2). Crucially, each output node can have its own LRP-process; for example, in a travel mode choice context, the ANN assigns a probability to each mode, representing the probability, for a particular case, that the traveller chooses, for instance, the bus, train, or car. LRP can then be used *for each of these probabilities*, to determine what factors were relevant for that prediction. In other words, LRP can be used to explain the choice probability, predicted by the ANN, for the bus mode, for the train mode, and for the car mode.

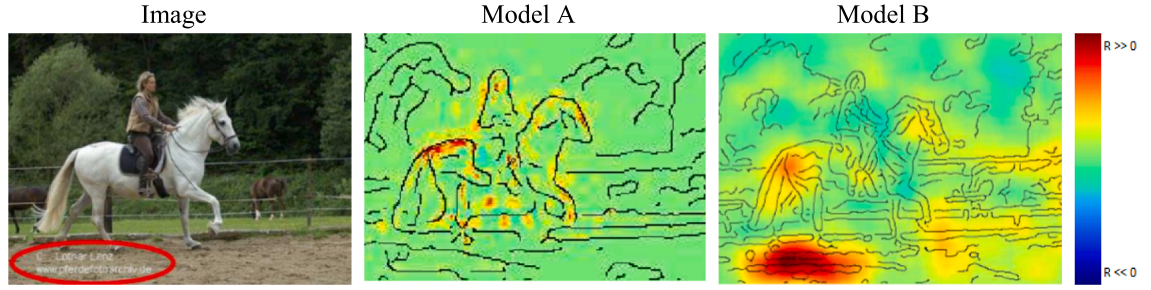


Fig. 3. Left: Image of the horse class, presented to two different models. Middle and right: relevance of each pixel is drawn as heat map. (For interpretation of the references to colour in this figure legend, the reader is referred to the online version of this article.)

However, in most cases the LRP method is applied to explain *the highest choice probability* assigned by the ANN; that is, the method explains why the ANN predicts that a particular mode has a higher probability than the others, of being chosen. In our paper, we use LRP in both ways, and we will clearly indicate when the method is used in which way.

The key property of the relevance redistribution process used in LRP is that the total relevance at every layer of the ANN (from the output layer to the input) needs to be maintained; this property is known as relevance conservation and can be described as follows:

$$\sum_i R_i = \dots = \sum_j R_j = \sum_k R_k = \dots = f(\mathbf{x}) \quad (1)$$

where i, j and k are the indices for nodes on the layers, and R_k is the relevance of node k for the relevance $f(\mathbf{x})$. This equation highlights that the method computes the decomposition of $f(\mathbf{x})$ (most right) in terms of the input variables (most left). To ensure Equation (1) holds, two rules need to be imposed:

$$\sum_j R_{j-k} = R_k \quad (2)$$

$$R_j = \sum_k R_{j-k} \quad (3)$$

where R_{j-k} is defined as the share of R_k that is redistributed to node j in the lower layer (see Fig. 2). The redistribution of the relevance resembles the process of forward propagation (used to produce predictions). In forward propagation, the activation function $z(\cdot)$ of the node k generates one output a_k that is fanned out to other neurons and can be described as follows (see Appendix A for comprehensive description of ANN structure):

$$a_k = z\left(\sum_j w_{jk} a_j + w_k\right) \quad (4)$$

where w_{jk} , w_k are the weight and bias parameter of the neuron. The main principle used by LRP to back propagate the relevance is that what has been received by a node should be redistributed to the nodes at the lower layer proportionally. In the literature, different ways in which relevance is back propagated have been proposed. Empirical studies have shown that some of these rules yield better relevance redistribution depending on many factors such as the used activation function and position of the hidden layer (i.e., the layer deepness). In this study, we use the ϵ -rule (as described in (Samek et al., 2019)), which back propagates the relevance to each neuron as follows:

$$R_j = \sum_k \left(\frac{w_{jk} a_j}{\sum_j (w_{jk} a_j) + \epsilon} \right) R_k \quad (5)$$

where ϵ is a fixed constant of small value ($\epsilon = 10^{-7}$) which is added to the denominator to prevent division by zero (not to be confused with the error in discrete choice models). Doing so avoids the relevance values to become too large. This equation shows that the relevance is propagated proportionally depending on: 1) the neuron activation a_j (i.e., more activated neurons receive larger share of relevance), and 2) the strength of the connection w_{jk} (more relevance flows through more strong connection). In this study, we focus only on rule shown in Equation (5), and for more detailed description of LRP and comprehensive discussion on alternative relevance redistribution rules, interested readers are referred to Samek et al. (2019) and Lapuschkin, Binder, Montavon, Müller, and Samek (2016).

2.3. Explaining a prediction using heat map - a computer vision illustration

To further clarify the method, in this subsection we provide a brief illustration of how the LRP method is commonly used in the

Table 2
Used performance metrics.

Performance metric	Function
Final Log-likelihood	$\sum_{n=1}^N \sum_{k=1}^K y_{nk} \ln(P_{nk})$
Cross-entropy	$-\frac{1}{N} \sum_{n=1}^N \sum_{k=1}^K y_{nk} \ln(P_{nk})$
ρ^2	$\rho^2 = 1 - \frac{LL(\hat{\beta})}{LL(0)}$

Table 3
Synthetic data specification and parametrisation.

Dataset no.	Model specification	Parametrisation	Cross-entropy (RUM-MNL)	ρ^2 (RUM-MNL)	Cross-entropy (ANN)	ρ^2 (ANN)
A1	$V_{in} = \sum_m \beta_m x_{imn}$	$\beta_1 = -6$ $\beta_2 = -4$	0.53	0.51	0.54	0.50
A2		$\beta_1 = +6$ $\beta_2 = +4$	0.53	0.51	0.54	0.50
A3		$\beta_1 = -6$ $\beta_2 = 0$	0.59	0.45	0.61	0.44

computer vision field. This particular example is taken from [Lapuschkin, Binder, Montavon, Muller, and Samek \(2016\)](#) whose aim is to explain the predictions of two different machine learning models (these models themselves are not of interest to us in this paper and are not discussed in any detail here). Each of these models is trained using large number of images to discriminate between several output classes, including a horse class. A horse image is presented to the two models, see the left-hand side plot in [Fig. 3](#). Both models produced the correct prediction with high confidence. Then, the prediction is propagated backward using the above-described explanation method (i.e., LRP) to provide an answer to the Why-question (why did the ANN believe that this is a picture of a horse). The analyst can then use the outcome of the LRP process to verify whether the model predictions are based on intuitive and expected rationales (the Domain Knowledge question). To facilitate inspection, the relevance is usually presented as a heat map, where pixels with high positive relevance are shown in red (see colour map on the right side of [Fig. 3](#)).

The middle and right-hand side plots in [Fig. 3](#) show the heat maps generated using the LRP method, given the input: the horse image on the left-hand side. Although the predictions produced by both models are correct, the heat maps reveal that the models have a different rationale. For a horse image, we expect (as human analysts with some domain knowledge) a well-trained model to base its prediction on relevant features and distinguishable characteristics of horses, such as e.g. the horse tail. [Fig. 3](#) shows that Model A indeed assigns a high relevance to such horse pixels, while Model B assigns a high relevance to the lower left-hand side corner of the image, where the copyright tag is located. Hence, the heat map reveals that the prediction of model B is largely based on the existence and nature of the copyright tag, rather than the part of the image where distinguishable characteristics of horse are shown. The source of this outcome is that in the training data many horse images were present with the same copyright tag. As a result, Model B has learned that the copyright tag is a good explanatory ‘variable’. This is a clear example of the fact that machine learning methods excel in detecting patterns, regardless of whether these patterns are meaningful, or not ([Abu-Mostafa, Magdon-Ismael, & Lin, 2012](#)). Most importantly for the purpose of this paper, this example illustrates that LRP can be used to inspect the model rationale and examine its trustworthiness, using human domain knowledge. In the following, we illustrate how the LRP can be recast and implemented for non-visual contexts, specifically discrete choice analysis (see the analogy between image classification and discrete choice modelling established earlier in this section).

2.4. Explaining a prediction in travellers’ discrete choice context – a re-conceptualisation using Monte Carlo experiments

This subsection conducts a series of Monte Carlo experiments to get a feeling for how heat maps can be re-conceptualised and used in the context of discrete choice data. Further, this part seeks to understand how heat maps results can be interpreted. [Table 3](#) shows the parametrisations of the three synthetic data sets that we generated. Each data set consists of three alternatives and two generic attributes: X_1 and X_2 . Parameters have different values across data sets (we use negative, positive and neutral parameter values). Each data set consists of 10,000 hypothetical respondents, each making a single choice. Attribute levels are generated using a random number generator between zero and one. To create the synthetic choices, the total utility of each alternative is computed and the highest utility alternative is assumed to be chosen, following a Logit (RUM-MNL) model where the random part of utility is distributed Extreme Value type I with variance $\pi^2/6$.

For each data set, a three-layers ANN with 4 hidden nodes on the hidden layers is trained. As has also been found in previous studies (e.g., [Alwosheel, van Cranenburgh, and Chorus \(2018\)](#)), the ANNs are able to learn the RUM-MNL data generating process with high accuracy, in the sense that the prediction performance of the ANN almost matches that of the true underlying data generating process encoded in a corresponding discrete choice model, as shown in [Table 3](#) (see [Table 2](#) for the used performance metrics).

For the first data set (A1), the negative sign of the parameters imposes a dislike for higher attribute values (i.e., the lower the attribute values, the more attractive the alternative becomes). Hence, the attribute values of the *chosen* alternative are expected to

Table 4
Results of observations randomly selected from A1 data set.

	Attribute Values						Relevance						True chosen alternative			ANN prob		
	X_1			X_2			X_1			X_2			Alt 1	Alt 2	Alt 3	Alt 1	Alt 2	Alt 3
	Alt 1	Alt 2	Alt 3	Alt 1	Alt 2	Alt 3	Alt 1	Alt 2	Alt 3	Alt 1	Alt 2	Alt 3						
Obs. 1	0.127	0.8887	0.916	0.038	0.871	0.742	Blue	Red	Red	Blue	Red	Red	1	0	0	0.99	0	0.01
Obs. 2	0.95	0.004	0.97	0.725	0.133	0.75	Red	Blue	Red	Red	Blue	Red	0	1	0	0.01	0.99	0
Obs. 3	0.936	0.957	0.045	0.882	0.866	0.157	Red	Red	Blue	Blue	Red	Blue	0	0	1	0.01	0	0.99

Table 5
Results of observations randomly selected from A2 data set.

	Attribute Values						Relevance						True chosen alternative			ANN prob		
	X_1			X_2			X_1			X_2			Alt 1	Alt 2	Alt 3	Alt 1	Alt 2	Alt 3
	Alt 1	Alt 2	Alt 3	Alt 1	Alt 2	Alt 3	Alt 1	Alt 2	Alt 3	Alt 1	Alt 2	Alt 3						
Obs. 1	0.97	0.19	0.06	0.95	0.07	0.107	Red	Blue	Blue	Blue	Blue	Blue	1	0	0	0.99	0.01	0
Obs. 2	0.108	0.98	0.0594	0.063	0.865	0.35	Blue	Red	Blue	Blue	Blue	Blue	0	1	0	0.01	0.99	0
Obs. 3	0.025	0.05	0.83	0.32	0.305	0.99	Blue	Blue	Red	Blue	Blue	Red	0	0	1	0.01	0	0.99

Table 6
Results of observations randomly selected from A3 data set.

	Attribute Values						Relevance						True chosen alternative			ANN prob		
	X_1			X_2			X_1			X_2			Alt 1	Alt 2	Alt 3	Alt 1	Alt 2	Alt 3
	Alt 1	Alt 2	Alt 3	Alt 1	Alt 2	Alt 3	Alt 1	Alt 2	Alt 3	Alt 1	Alt 2	Alt 3						
Obs. 1	0.05	0.665	0.979	0.99	0.001	0.757	Blue	Blue	Red	Blue	Blue	Blue	1	0	0	0.98	0.1	0.1
Obs. 2	0.97	0.05	0.99	0.323	0.385	0.329	Red	Blue	Blue	Blue	Blue	Blue	0	1	0	0.01	0.99	0
Obs. 3	0.98	0.9	0.00038	0.017	0.154	0.94	Red	Red	Blue	Blue	Blue	Blue	0	0	1	0	0.01	0.99

contribute negatively to the choice probability prediction for that alternative (as reducing the attribute values would increase the attractiveness of the chosen alternative). In contrast, we expect that high attribute values of the *non-chosen* alternatives contribute positively to the prediction, implying that the attractiveness of these non-chosen alternatives increases as these attribute values increase. These expectations are confirmed in Table 4, where we see the relevance of the attribute values that are computed using the LRP method⁴, alongside the choice probabilities predicted by the ANN, for three randomly selected observations from the synthetic data. In this Table, we apply the LRP method to explain the choice probability assigned to the chosen alternative – that is, we do not explain choice probabilities assigned to non-chosen alternatives. In the heat map positive relevance values are depicted red; negative relevance values are depicted blue, and neutral relevance (or: irrelevance) values are depicted white. The colour intensity for each observation is normalised to the maximum absolute value.

Consider the three observations shown in Table 4, where alternative 1 is chosen in the first observation, alternative 2 is chosen in the second observation, and alternative 3 is chosen in the third observation. Note that the ANN predictions are correct with very high confidence as shown by predicted choice probabilities of 0.99 for the chosen alternative in each of the three observations. The blue diagonal values show, as expected given the negative signs of the true parameters, that the attribute values of the chosen alternative have contributed negatively toward the predicted probability of the alternative being chosen. In contrast, the off-diagonal cells, which here are associated with the non-chosen alternatives, are coloured red. This means that the attribute values of these unattractive alternatives, which are comparatively high, positively contribute to the prediction that alternative 1 is chosen in observation 1, alternative 2 in observation 2, etc. This heat map or colouring scheme is thus completely in line with what the analyst would expect, given the data generating process.

Compared to the first data set, in the second data set (A2) the parameters have flipped signs. Hence, lower attribute values are more attractive than higher ones. Table 5 shows the results for three randomly selected observations (again, from the subset of observations that are correctly predicted by the ANN). We use same colour map and intensity as in Table 4. As can be seen, Table 5 reveals the same patterns as shown in Table 4, but colours are flipped, i.e., cells on the diagonal are now red, and cells off the diagonal are now blue. This is fully in line with expectations, as here an increase (decrease) in the attribute levels of the chosen (non-chosen) alternative positively contributes to the choice probability that is predicted for the chosen alternative.

Lastly, Table 6 presents the results for data set A3. Again, three randomly selected observations from the subset of observations that are correctly assigned by the ANN are shown. In this data set, β_2 is zero. This means that the attribute X_2 does not impact the decision makers' choices in the data generation process. As such, we expect the relevancies for these attribute values to have values that are close to zero. In line with expectation, Table 6 shows that all cells for X_2 are (almost) white – meaning that the values of this attribute do neither positively or negatively contribute to the predicted choice probabilities.

In sum, this application on synthetic data provides a first idea of how the LRP method can be used to inspect the rationale based on which an ANN makes its predictions in a travel mode choice context, and it provides a first sign of face validity of the method. The next

⁴ To generate heat maps, the LRP method is used and implemented in the Python environment using the open source library iNNvestigate (Alber et al., 2019).

Table 7
Data statistics.

No.	Attribute	Description	Type	Range [min, max]	Mean and standard deviation
1	TC_{Drive}	Estimated cost of driving route, including fuel cost and congestion charge	Float (£)	[0.05, 17.16]	(1.91, 3.48)
2	TC_{PubTr}	Estimated cost of public transport route, accounting for rail and bus fare types	Float (£)	[0, 13.49]	(1.56, 1.55)
3	TT_{Drive}	Predicted duration of driving route	Float (minutes)	[0.02, 142]	(17, 15)
4	TT_{PubTr}	Predicted duration of public transportation	Float (minutes)	[0.02, 141]	(28, 19)
5	TT_{Walk}	Predicted total duration of walking times for interchanges on public transport route	Float (minutes)	[0.02, 550]	(69, 68)
6	DIS	Straight line distance between origin and destination	Integer (meters)	[96, 40,941]	(4,690, 4,827)
7	$TRAF$	Predicted traffic variability on driving route	Float	[0, 1]	(0.34, 0.20)
8	$INTER$	Number of interchanges on public transport route from directions API	Integer	[0, 4]	(0.38, 0.62)
9	DL	Boolean identifier of a person making trip: 1 if person has driving license, 0 otherwise	Bool	[0, 1]	(0.62, 0.49)
10	CO	Car ownership of household person belongs to: no cars in household (0), less than one car per adult (1), one or more cars per adult (2)	Integer	[0, 2]	(0.99, 0.75)
11	FEM	Boolean identifier of a person making trip: 1 if female, 0 otherwise	Bool	[0, 1]	(0.53, 0.49)
12	AG	Age of person making trip	Integer (years)	[5, 99]	(39.5, 19.3)

sections present an application of the method on a real empirical data set.

3. Empirical data and ANN training

3.1. Data preparation

For this study, we use revealed preference (RP) data from a study conducted for travel mode choice analysis in London city (Hillel, Elshafie, & Jin, 2018).⁵ This dataset contains of four alternatives, and a total of 27 features (i.e., attributes of alternatives and characteristics of decision makers). Three processing steps have been executed to prepare the data for this study: First, features that were considered redundant are removed, or merged with others. For instance, rather than using three features to represent car cost (fuel, congestion, and total cost), we merged them into a single one representing the total car cost. Table 7 shows statistics on the attribute levels in the dataset used for this analysis. Second, we noticed that the dataset is highly imbalanced in terms of the chosen mode: walking (17.6%), cycling (3.0%), public transport (35.3%) and driving (44.2%). Such imbalances could affect the reliability of the trained ANNs (Haykin, 2009). As this paper is concerned with explaining ANN predictions (i.e., we do not aim to find the best ANN to predict the mode choices), we considered dealing with this sort of data imbalances out of scope for this paper. Therefore, the data imbalance is ‘repaired’ by eliminating the cycling alternative from the dataset.⁶ Third, we excluded very short trips (i.e., less than two minutes), as these were deemed not to contain a mode trade-off. The resulting dataset that is used for this study consists of 77,638 mode choice observations.

3.2. ANN development and training

The ANN is implemented in a Python environment, using the open source deep learning library Keras (Chollet, 2015). The ANN is trained based on so-called cross-entropy cost function (see Table 2). Note that minimising the cross-entropy is equivalent to maximising the log-likelihood (see e.g. (Bishop, 1995)). To update weights’ values w , the built-in algorithm known as Adam is used

⁵ The dataset and its description are available online, and can be downloaded from the first author profile at researchgate.net

⁶ It is well known, that under-representation of particular alternative can undermine the reliability of a trained ANN model. However, a plethora of methods and approaches are developed to combat these issues. For example, a commonly used approach is to synthesise more observations of the under-represented alternative (see e.g., (Chawla, Bowyer, Hall, & Kegelmeyer, 2002)). Another approach is based on penalising the ANN when it makes classification mistakes concerning the under-represented alternatives. For further discussion on these methods, interested readers are referred to e.g. (He & Garcia, 2008) and (Batista, Prati, & Monard, 2004).

Table 8
Performance of the trained ANN.

Performance metric	Null model	ANN	Linear-additive RUM
Final Log-likelihood	-86,625	-43,477	-50,704
Cross-entropy	1.09	0.56	0.65
ρ^2	0	0.50	0.42

Table 9
Confusion matrix.

		ANN Classification			
		Driving	Public Transport	Walking	Σ
True chosen alternative	Driving	82.55 (0.69)	11.23 (0.19)	6.22 (0.10)	100% (1)
	Public Transport	21.22 (0.25)	72.66 (0.66)	6.12 (0.09)	100% (1)
	Walking	23.72 (0.25)	11.56 (0.17)	64.72 (0.57)	100% (1)

Table 10
Results of observation 1 (index: 47,489 and true chosen alternative is Drive).

	Alternatives' Characteristics						Other Characteristics		
	Alt.1: Drive	Alt.2: PubTr	Alt.3: Walk	Alt.1: Drive	Alt.2: PubTr	Alt.3: Walk	Attribute	Value	Relevance
	Attribute value			Relevance					
TT (min)	23.48	137	160				AG	47	
TC (£)	1.58	7.50					FEM	0	
TRAF	0.03						DL	1	
INTER		4					CO	2	
ANN probs	0.99	0	0.01				DIS	9,556	

Table 11
Results of observation 2 (index: 24,618 and true chosen alternative is Walk).

	Alternatives' Characteristics						Other Characteristics		
	Alt.1: Drive	Alt.2: PubTr	Alt.3: Walk	Alt.1: Drive	Alt.2: PubTr	Alt.3: Walk	Attribute	Value	Relevance
	Attribute value			Relevance					
TT (min)	7.38	4	6				AG	26	
TC (£)	10.70	2.40					FEM	1	
TRAF	0.31						DL	1	
INTER		0					CO	0	
ANN probs	0	0.01	0.99				DIS	368	

(Kingma & Ba, 2014). Prior to training the ANN, the data are normalised to reduce training time and minimise the likelihood of ending-up with suboptimal local solutions.⁷ A conventional three layers (input, output and one hidden layer consist of ten nodes, see Appendix A for a similar ANN layout) fully connected ANN structure is used. Unlike the traditional three-layers ANN, we have removed the bias nodes in the hidden and output layer to avoid losing fraction of the relevance values.⁸ Note that the bias nodes removal has not impacted the prediction performance of the trained ANN. To train the ANN and test its performance to predict the travel mode choice, we conducted a so-called *k*-fold cross-validation method, with *k* = 5. The data set is randomly partitioned into five equally sized folds of (roughly) 15,528 observations. Then, a single fold is used for testing, while the remaining four folds are used for training. This process is repeated 5 times, where each of the five folds is used only once for testing.

Table 8 shows several performance metrics for the trained ANN. The reported performance metrics are averaged across the five hold-out folds. It shows that ANN achieves a satisfactory prediction performance. We also report the performance of a standard linear-additive RUM-MNL model (see Appendix B for the model specifications).⁹ Note that presenting the ANN and RUM-MNL results in

⁷ Data normalisation is a common practice for ANN training. In this study, the minimum and maximum values of data are normalised to 0 to +1.

⁸ ANN complexity is adjusted using a cross validation approach (see (Alwosheel et al., 2018) for more details). To avoid overfitting, a commonly used rule-of-thumb in ANNs is that the sample size needs to be (at least) 10 times larger than the number of adjustable parameters in the network (Haykin, 2009). A recent study specifically dealing with sample size requirements for using ANNs in the context of choice models is more conservative, and recommends to use a sample size of (at least) 50 times the number of estimable weights (Alwosheel et al., 2018). Our sample size satisfies this condition and, therefore, we safely avoid overfitting issues.

⁹ Note that the *k*-fold method is not used for the RUM model. Rather, the RUM model is estimated one time using the whole dataset.

Table 12
Results of observation 3 (index: 1,621 and true chosen alternative is Walk).

	Alternatives' Characteristics						Other Characteristics		
	Alt.1: Drive	Alt.2: PubTr	Alt.3: Walk	Alt.1: Drive	Alt.2: PubTr	Alt.3: Walk	Attribute	Value	Relevance
	Attribute value			Relevance					
TT (min)	7.23	22	24				AG	15	
TC (£)	0.30	0.00					FEM	1	
TRAF	0.44						DL	0	
INTER		0					CO	1	
ANN probs	0.33	0.33	0.34				DIS	1,271	

Table 8 does not mean that we intend to compare the two models. RUM-MNL is estimated here because it is used in the next Section to guide the selection of observations to analyse using the LRP method (see Section 4.2). Table 9 shows the *k*-folds confusion matrix for the trained ANN. To construct the confusion matrix each observation is assigned to an alternative based on the highest probability as predicted by the ANN. Then, each prediction is compared to the true chosen alternative. The cells on the diagonal show the mean percentage of the observations that are correctly assigned, across the 5 folds. Additionally, the values between parentheses show the average ANN probabilities of the observations that are correctly classified. The off-diagonal cells show the mean percentage of observations that are misclassified, across the 5 folds. Values between parentheses show the average ANN probabilities of these observations.

4. Applying the LRP method

4.1. ANN prediction explanation of randomly selected observations

In this subsection, we use the LRP-generated heat maps for multiple observations with the aim to understand *why* the ANN produces certain mode choice predictions. Tables 10-12 show the back-propagated relevance extracted for three observations randomly selected from the subset of observations that are correctly assigned by the ANN. It can be seen, that predictions are made with different levels of confidence. In the context of our analyses, a high confidence level means the network assigns a choice probability of more than 0.80 to one the modes, and a low confidence level means that the highest (across travel mode alternatives in the context of a particular observation) predicted choice probability is still below 0.40. As such, for diversification purposes and to build trust in the model as a whole, the three observations are randomly selected as follows: two predictions with high confidence levels and one prediction with low confidence level. Tables 10-12 show the ANN probabilities, the attributes' values, and relevancies obtained using LRP for the selected observations. A heat map (using the same colour coding as in section 2.4 i.e., positive, negative and neutral values are depicted in red, blue and white, respectively) is employed to visualise the relevancies. As in the Monte Carlo analysis, we apply the LRP to the output node with the highest (choice) probability.

Table 10 shows an observation of a middle-aged female, who holds a driver license and owns two cars, who chose the driving alternative, which indeed seems to be the most attractive travel alternative in this case as is the fastest and cheapest alternative. In line with intuition, the ANN predicts a choice for the driving alternative with a very high level of confidence (assigning a 0.99 choice probability to that alternative). The relevance values show that car travel time receives a strong negative relevance, as expected (given that lower travel times are preferred). The relatively long travel times offered by the non-chosen alternatives receive a strong positive relevance, as expected (given that the high travel times of these alternatives makes driving alternative more appealing). Furthermore, the number of owned cars (two) and the driving license availability have a positive relevance. Together, these analyses reveal on what basis the ANN model has predicted that this traveller would choose the driving alternative. From a travel behaviour perspective, all these points are in line with expectations. As such, an analyst equipped with the proper domain knowledge should trust (the rationale behind) this prediction.

Moving forward to Table 11, for this observation, a young female traveller chose the walking alternative. As before, the travel time and cost of the non-chosen alternatives and the relatively high traffic on the driving route have high positive relevance for the predicted choice probability for walking. Furthermore, we see that the travel time of the chosen alternative, and the travelled distance have negative relevance values. All these relations are expected from a travel behaviour perspective; hence, this prediction too can be safely trusted. Lastly, in Table 12 the alternative with highest predicted probability is walking; however, this mode receives a predicted probability which is only one percentage point higher than that of the other mode, implying that the ANN has low confidence in this prediction. The relevance values show that attribute values with negative relevance for the predicted choice probability for the walking alternative, are the relatively long distance and walking travel time, suggesting that shorter distance and less walking time would have made the walking alternative more attractive. This is expected from a travel behaviour perspective. Further, it can be noticed that the red and blue colours associated in this heat map are less bright, meaning that the ANN is less outspoken about what determined its prediction; this too is to be expected, given that the ANN assigns almost equal choice probabilities to each of the three alternatives.

Table 13

Classes depicting incorrect ANN and RUM-MNL predictions. Values between parenthesis are the total number of observations for each case.

		RUM-MNL prediction	
		Correct	Incorrect
ANN prediction	Correct		Class I (6,679)
	Incorrect	Class II (3,588)	Class III (14,792)

Table 14

Results of first observation in Class I (index: 7,011 and true chosen alternative is Walking).

	Alternatives' Characteristics						Other Characteristics		
	Alt.1: Drive	Alt.2: PubTr	Alt.3: Walk	Alt.1: Drive	Alt.2: PubTr	Alt.3: Walk	Attribute	Value	Relevance
	Attribute value			Relevance					
TT (min)	5.32	5	7				AG	18	
TC (£)	0.22	1.50					FEM	1	
TRAF	0.02						DL	0	
INTER		0					CO	2	
ANN probs	0.06	0.01	0.93				DIS	403	
RUM probs	0.47	0.14	0.39						

Table 15

Results of second observation in Class I (index: 38,475 and true chosen alternative is Driving).

	Alternatives' Characteristics						Other Characteristics		
	Alt.1: Drive	Alt.2: PubTr	Alt.3: Walk	Alt.1: Drive	Alt.2: PubTr	Alt.3: Walk	Attribute	Value	Relevance
	Attribute value			Relevance					
TT (min)	3.92	9	22				AG	18	
TC (£)	0.21	0.00					FEM	0	
TRAF	0.14						DL	0	
INTER		0					CO	1	
ANN probs	0.35	0.33	0.32				DIS	1,158	
RUM probs	0.3	0.43	0.29						

Table 16

Results of Class II observation (index: 32,923 and true chosen alternative is Public Transport).

	Alternatives' Characteristics						Other Characteristics			
	Alt.1: Drive	Alt.2: PubTr	Alt.3: Walk	Alt.1: Drive	Alt.2: PubTr	Alt.3: Walk	Attribute	Value	Relevance	Relevance from true alt
	Attribute value			Relevance			Relevance from true alt			
TT (min)	58.98	61	206				AG	5		
TC (£)	13.21	0.00					FEM	1		
TRAF	0.71						DL	0		
INTER		2					CO	2		
ANN probs	0.59	0.4	0.01				DIS	14,764		
RUM probs	0.01	0.98	0.01							

4.2. Using RUM-MNL and ANN models to guide observation selection

In this subsection, we use RUM-MNL (a highly robust and well understood model for travel mode choice analysis) and ANN predictions jointly to guide the process of observations selection, instead of relying on ANN predictions only, as in the previous subsection. This allows us to examine the overall workings and rationale of the trained ANN and decide whether we can trust a trained ANN as a whole. Furthermore, we in this section analyse correct as well as incorrect predictions. Note that while explaining correct predictions made by the black-box is important (as shown in previous subsection), it could even be more important to inspect why an ANN makes particular wrong predictions. This would help to obtain a higher level understanding on the model. Specifically, we are interested to learn whether, or not, these wrong predictions are based on meaningful intuition, or on counter intuitive or flawed relations learned by the ANN. It goes without saying that a mis-prediction by a trained ANN does not necessarily mean it has learned counterintuitive or flawed relations; just like a mis-prediction by a classical choice model like the MNL model would not invalidate that model. But, if the ANN has learned spurious or otherwise counter-intuitive relations, those are particularly likely to show up in mis-

Table 17
Results of Class III first observation (index: 48,999 and true chosen alternative is Walking).

	Alternatives' Characteristics									Other Characteristics			
	Alt.1: Drive			Alt.2: PubTr			Alt.3: Walk			Attribute	Value	Relevance	Relevance from true alt
	Attribute value	Relevance	Relevance from true alt	Attribute	Value	Relevance	Relevance from true alt						
TT (min)	11.60	38	59						AG	72			
TC (£)	0.61	3.00							FEM	0			
TRAF	0.10								DL	1			
INTER		1							CO	2			
ANN probs	0.99	0	0.01						DIS	2,861			
RUM probs	0.98	0.02	0										

predictions.

To select a diverse set of observations (including observations where the trained ANN makes a wrong prediction), we distinguish between three classes, see Table 13. For each class, we randomly sample one or a few observations to analyse using LRP-generated heat maps.

- Class I: The ANN model predicts the true chosen alternative, while the RUM-MNL model makes the wrong prediction. For this case, we randomly select two observations: one for ANN prediction with high probability, and the other for ANN prediction with low probability (see Tables 14 and 15).
- Class II: The RUM-MNL model predicts the true chosen alternative, while the ANN misses it. For this case, we randomly select one observation (see Table 16). As explained in 2.2, relevance back-propagation using the LRP method can be implemented for any node at the network. In addition to having the relevance for the predicted alternative, we for this class also compute the relevance for the true chosen alternative (which the ANN misses), which allows for additional examination of the black-box rationale.
- Class III: Both the ANN and the RUM-MNL model mis-predict the correct alternative. Under this category, there are two subcases: ANN and RUM model agree (e.g., an observation where both models predict Driving, and the true chosen alternative is Walking), or ANN and RUM disagree (e.g., an observation where the true chosen alternative is Walking, ANN prediction is Public Transport, RUM prediction is Driving). One observation is selected for each subcase. See Tables 17 and 18 for the selected observations details.

Tables 14 and 15 show (for Class I observations) the attribute values, the relevancies produced using the LRP method, and the ANN and RUM-MNL choice probabilities. Table 14 shows a young female who lives in a household where two cars are owned; she chose the walking alternative. For the chosen alternative, the attribute values with negative relevance in the context of the ANN model are the distance and walking travel time. Further, the travel time values of the non-chosen alternatives have resulted in positive relevance values. Both of these points are in line with expectations and have been also noted from the observation shown in Table 12 (where the walking alternative was also predicted). For the observation shown in Table 15, the relatively long distance, and longer travel time offered by public transport and walking alternatives have a positive relevance for the prediction of driving, as we expect.¹⁰ Further, also in line with expectations, travel time and cost of the chosen alternative have a negative relevance to the prediction.

It is possible to end up with relevance values that are unexpected or hard to rationalise. For instance, we expect owning a car to have a positive relevance for the choice probability predicted for the driving alternative, but that is not always the case, as the observation shown in Table 15 reveals. Also, the unavailability of driving license only has a negligible contribution to the driving prediction. It should be kept in mind here that, since the ANN itself is a probabilistic technique that is not expected to fit complex data perfectly (Abu-Mostafa et al., 2012), we should not expect the relevance values that are produced by LRP to always provide a fully accurate description of the contribution of all independent variables on every observation. As such, we advise the analyst to tolerate having some unexpected relevancies' values, but of course (s)he has the 'final say' on deciding to what extent these unexpected relevancies are tolerable or not – leading to a rejection of the trained network in the latter case. For this particular prediction (shown in Table 15), we believe having two unexplainable values (out of 11) is acceptable, given that all other values are in line with expectations based on domain knowledge, and in light of the fact that the ANN indicates a low level of confidence in this particular prediction.¹¹

Two back-propagated relevancies are extracted for Class II observation, where the RUM-MNL model predicts the true chosen alternative (public transport), and the ANN incorrectly predicts that the driving alternative has the highest choice probability. For a deeper examination of the trained ANN rationale, Table 16 shows the relevance values back-propagated from two output nodes: one for the public transport alternative (the true chosen alternative), and another for the driving alternative (which was predicted by the ANN to have the highest choice probability). By doing so, we can obtain a higher level of trust in the model, as we are now able to inspect the model reasoning in the case of "mis-prediction" (i.e., we may come to understand what has led the model to mis-predict, and whether this is still based on an intuitive and defensible rationale). For instance, the relevancies of driving alternative shows that relatively high travel times of the other two alternatives have led to the driving prediction, which is to be expected. Further, the high travel cost and time of the predicted alternative have negative contributions, which is also in line with domain knowledge. Inspecting

¹⁰ Note that the driving alternative also includes car passenger, van, taxi and motor bike (see T. Hillel et al. (2018) for more information).

¹¹ A similar pattern can be also noticed in the computer vision example (presented in subsection 2.3). For instance, we can identify small red spots on non-horse pixels (i.e., pixels showing the background, see Fig. 3).

Table 18
Results of Class III second observation (index: 46,900 and true chosen alternative is Walking).

	Alternatives' Characteristics									Other Characteristics			
	Attribute value			Relevance			Relevance from true alt			Attribute	Value	Relevance	Relevance from true alt
	Alt.1: Drive	Alt.2: PubTr	Alt.3: Walk	Alt.1: Drive	Alt.2: PubTr	Alt.3: Walk	Alt.1: Drive	Alt.2: PubTr	Alt.3: Walk				
TT (min)	14.38	9	38							AG	34		
TC (£)	0.56	2.40								FEM	0		
TRAF	0.57									DL	0		
INTER		0								CO	0		
ANN probs	0.49	0.42	0.09							DIS	3,272		
RUM probs	0.24	0.61	0.15										

the relevance extracted from the true chosen alternative (public transport), we observe that the long travel time and the high number of owned cars have contributed negatively to the choice probability assigned to the public transport alternative, highlighting that the probability of choosing public transport would have been higher if these values are lowered, which is as expected. In sum: despite that the ANN fails to make the correct prediction for this case and despite that the RUM-MNL model is able to correctly predict the chosen alternative, we find no evidence that the ANN's mis-prediction is rooted in a fundamental misreading of the choice situations at hand.

Finally, two back-propagated relevancies are presented for the two scenarios of Class III (Table 17 shows a case where the ANN and RUM models agree, and Table 18 shows a case where the two models disagree). In Table 17 (where both the ANN and RUM models predict a choice for the driving alternative with high confidence), the chosen alternative is walking, despite that the travelled distance is relatively long (around 3 km). This indicates that in this particular case, the actual choice for the walking alternative deviates from expectations regarding the length of the average walking trip. The produced relevancies for the ANN are actually as expected. For example, the relevance computed for the actually chosen alternative (walking) shows that walking travel time and distance have the highest negative relevance, indicating that the walking probability would have been higher if walking travel time and distance were both lower – this makes sense. A similar point can be also noted for relevancies shown in Table 18 (where the RUM and ANN models disagree). Also here, the true chosen alternative is walking, despite the relatively long travel time and distance. The back-propagated relevancies of these two attributes from the walking node are negative, explaining the reasons for this mis-prediction which turn out to be in line with common sense and domain knowledge.

5. Conclusions and recommendations

Using a series of Monte Carlo experiments, this study re-conceptualises the use of heat maps, generated using a Layer-wise Relevance Propagation method, to explain predictions of Artificial Neural Networks in the context of travel choice analysis. First, we illustrate the approach using simulated data, taking a first step towards face validity. Then, by analysing a recently collected real data set, we show how heat maps can be practically applied to provide explanations behind particular predictions of a trained ANN, thereby helping an analyst to build trust in those predictions. Additionally, we show that by carefully selecting a set of observations and associated predictions, the LRP method can ultimately help building trust in a trained ANN as a whole (or not, in which case the ANN can be retrained, adapted or discarded altogether). Our results suggest that the proposed approach provides a valuable addition to the toolbox of analysts who plan to use ANNs for choice modelling in general or travel demand analysis purposes in particular.

We would like to point out several limitations to this study, providing potential directions for future research. Firstly, to generate heat maps, this study implemented the widely used LRP rule. Several alternative variations to this rule have been proposed in the literature, and some are found to provide even better outcomes in specific domains (e.g., natural language processing). Investigating the performance of these alternative rules in the context of transport applications is a fruitful direction for further research. Possibly, this could lead to the discovery of new rules that particularly work well for transportations contexts. Secondly, additional to explaining ANN predictions, it is possible to use the LRP technique in hidden nodes to reveal what concepts and features have been learned by the trained ANN (several researches (e.g., (Olah et al., 2018)) have investigated this in a computer vision context). We believe doing so in travel choice behaviour context may provide a deeper understanding of the workings of ANNs and perhaps even of the latent decision-making processes of travellers. Thirdly, the empirical analyses provided in this paper are based on a single empirical data set and a Monte Carlo analysis on synthetic data. It is advisable to repeat these analyses on more data sets with different characteristics (e.g., more and different attributes and alternatives). This will provide a richer view on the generalisability of the proposed method to explain ANNs' predictions. Fourthly, the data imbalances problem exists in the used empirical data set is 'repaired' by removing the least represented alternative (i.e., cycling). Although we believe doing so has led to a more balanced situation, a future research direction may include analysing more data sets where imbalances issues are of less concern. Fifthly, to build trust in the ANN model as a whole, predictions of RUM-MNL and ANN models are used to guide the observation selection process. Although we believe this process is very helpful to select diverse observations, it might be rewarding to develop alternative selection strategies that may result in an even

better representation of the data set. Lastly, in addition to the proposed approach, an interesting avenue for research would be to inspect ANN trained on travel choice data using alternative elucidation approaches (e.g. alternative back-propagation or attribution approaches, see (Ribeiro, Singh, & Guestrin, 2016) for examples).

To conclude, while our analysis suggests that the proposed LRP-based heat map methodology provides a valuable tool to understand the rationale behind ANN predictions in the context of travel choice behaviour, it is important to acknowledge that the proposed method does not completely solve the ANNs' black-box issue as it will never completely explain the inner workings of the network. In our view and despite ongoing advances in explainable ANNs, their most natural domain of use in transportation still remains in applications where complete model transparency is not a prerequisite and analyst aims for high prediction performance (as oppose to e.g. deriving solid welfare-economic implications). Finally, we wish to note that the LRP-based heat map methodology has shown a great success in improving the explainability of trained ANNs' predictions in various contexts (e.g. sentiment analysis); hence it has the potential to be also implemented in other transportation contexts beyond the travel demand analysis and travel choice behavior contexts.

CRedit authorship contribution statement

Ahmad Alwosheel: Conceptualization, Methodology, Software, Writing - original draft. **Sander Cranenburgh:** Supervision, Investigation, Validation, Writing - review & editing. **Caspar G. Chorus:** Supervision, Investigation, Validation, Writing - review & editing.

Acknowledgment

The third author would like to acknowledge funding from ERC, consolidator grant BEHAVE – 724431.

Appendix A. . Artificial Neural Networks – An overview

ANNs consist of highly interconnected processing elements, called neurons, which communicate together to perform a learning task, such as classification, based on a set of observations. Fig. A1 shows the layout of the neuron structure.

Each neuron in the network receives inputs (t_m) multiplied by estimable parameters known as weights (w_m). The weighted inputs are accumulated and added to a constant (called bias, denoted b) to form a single input v for a pre-defined processing function known as activation function $z(\cdot)$. The bias has the effect of increasing or decreasing the net input of the activation function by a constant value, which increases the ANNs flexibility (Haykin, 2009). The activation function $z(\cdot)$ generates one output a that is fanned out to other neurons. The output a can be described as follows:

$$a = z(v) = z\left(\sum_{m=1}^M w_m * t_m + w_b\right), \text{ where } w_b \text{ is the weight associated with the bias.}$$

The neurons are connected together to form a network (Bishop, 2006; LeCun, Bengio, & Hinton, 2015). A widely used ANN structure consists of layers of neurons connected successively, known as multi-layer perceptron (MLP) structure. Typically, the first (input) layer and the output layer depend on the problem at hand. More specifically, input layer neurons represent the independent variables. In the context of choice modelling, these are the alternatives' attributes, characteristics of decision-makers, and contextual factors. The output layer, in a discrete choice context, consists of neurons that provide choice probabilities P for each alternative. Layers in-between are called hidden layers because their inputs and outputs are connected to other neurons and are therefore 'invisible' to the analyst. For illustrative purposes, consider the following hypothetical situation: a person can travel using one of three modes: bus, train, or car; two attributes (travel cost "TC" and travel time "TT") are associated with each alternative. Fig. A2 shows this typical choice situation in a three-layer MLP network with four hidden neurons (Alwosheel et al., 2017).

Neurons at the hidden and output layers are represented by circles in Fig. A2, while input and bias neurons are represented by squares. This is to emphasise that the neurons at the hidden and output layers are processing units, meaning that they receive inputs t and return outputs a according to predefined activation function $z(\cdot)$, as illustrated in Fig. A1. Input neurons pass the input signals to the next layer. In Fig. A2, the ANN has a total of 7 processing units.

For a complete MLP structure, three elements need to be defined:

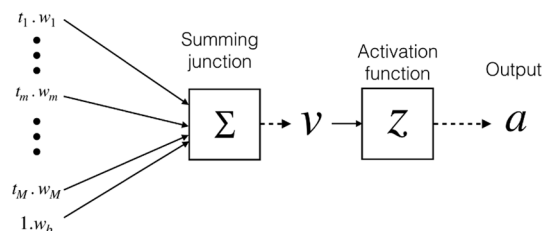


Fig. A1. A neuron layout.

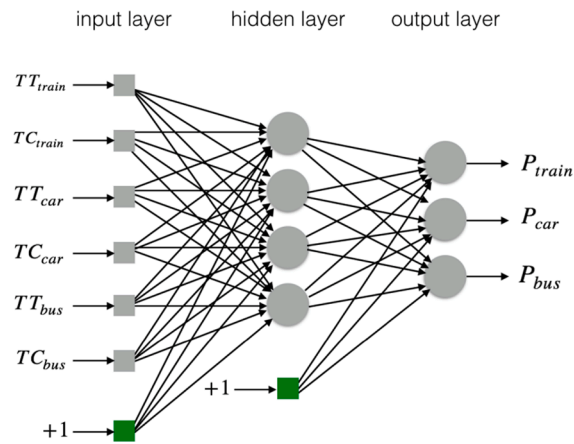


Fig. A2. Three-layers Artificial Neural Network.

- (1) Number of hidden layers: a commonly used structure is three-layers MLP: input, output and one hidden layer. A key property of this structure lies in the ability to approximate, with arbitrary level of precision, any measurable function given that a sufficient number of processing neurons are available at the hidden layer; this property is known as the Universal Approximation Theorem (UAT) (Cybenko, 1989; Hornik, Stinchcombe, & White, 1989).
- (2) Number of neurons for the hidden layer(s): the UAT holds true only if a sufficient number of hidden neurons are available. Intuitively, ANNs with more hidden neurons have more free parameters (w) and are therefore capable of learning more complex functions.
- (3) Activation function $z(\cdot)$: As mentioned before, each neuron processes its input via a pre-defined activation function. Neurons at the same layer usually employ identical functions. In the analyses presented in the remainder of this paper, a tangent sigmoidal function has been employed at the hidden layer neurons, as it has been shown to lead to fast training times (LeCun, Bottou, Orr, & Müller, 2012). For the output layer, a so-called softmax function is used (which is essentially a logit) to ensure that the sum of the choice probabilities equals one.

Appendix B. . Specifications of the linear-additive random utility maximisation model

Table A1 shows the estimation results of the linear-additive random utility maximisation (RUM) model used in this study (see Table 1 for attributes’ name, notation, and description). The model is estimated in Multinomial Logit (MNL) form.. As can be seen, and as is expected, all parameters have the intuitively correct sign and are highly significantly different from zero. Table A2 shows the observed utility function for RUM model.

Table A1
Estimation results for RUM-MNL model.

No. of observations	77,638	
Final LL	-50,716.29	
ρ^2	0.41	
Attribute	Est.	Rob. t-values
ASC_Drive	0	fixed
ASC_PubTr	1.81	59.60
ASC_Walk	2.64	74.47
TT	-6.10	-95.31
TC	-0.135	-8.85
DL	1.02	46.26
CO	1.38	89.96
INTER	0.765	37.99
TRAF	-2.70	-43.44
AG_TC	-0.128	-4.04
DIS_TC	0.00937	11.59
FEM_TC	-0.0377	-4.31

Table A2

Utility function specifications.

$$\begin{aligned}
 V_{Drive} &= ASC_{Drive} + \beta_{TT}TT_{Drive} + \beta_{TC}TC_{Drive} + \beta_{AG_TC}(AG^*TC_{Drive}) + \beta_{DIS_TC}(DIS^*TC_{Drive}) + \beta_{FEM_TC}(FEM^*TC_{Drive}) + \beta_{DL}DL + \beta_{CO}CO + \beta_{TRAF}TRAF \\
 V_{PubTr} &= ASC_{PubTr} + \beta_{TT}TT_{PubTr} + \beta_{TC}TC_{PubTr} + \beta_{AG_TC}(AG^*TC_{PubTr}) + \beta_{DIS_TC}(DIS^*TC_{PubTr}) + \beta_{FEM_TC}(FEM^*TC_{PubTr}) + \beta_{INTER}INTER \\
 V_{Walk} &= ASC_{Walk} + \beta_{TT}TT_{Walk} + \beta_{TC}TC_{Walk} + \beta_{AG_TC}(AG^*TC_{Walk}) + \beta_{DIS_TC}(DIS^*TC_{Walk}) + \beta_{FEM_TC}(FEM^*TC_{Walk})
 \end{aligned}$$

References

- Abu-Mostafa, Y. S., Magdon-Ismael, M., & Lin, H.-T. (2012). Learning from data (Vol. 4): AMLBook New York, NY, USA.
- Adebayo, J., Gilmer, J., Muelly, M., Goodfellow, I., Hardt, M., Kim, B., 2018. Sanity checks for saliency maps. Paper presented at the Advances in Neural Information Processing Systems.
- Alber, M., Lapuschkin, S., Seegerer, P., Hägele, M., Schütt, K.T., Montavon, G., Kindermans, P.-J., 2019. inNvestigate neural networks! J. Mach. Learn. Res. 20 (93), 1–8.
- Alwosheel, A., van Cranenburgh, S., Chorus, C., 2017. Artificial neural networks as a means to accommodate decision rules in choice models. Paper presented at the International Choice Modelling Conference 2017.
- Alwosheel, A., van Cranenburgh, S., Chorus, C.G., 2018. Is your dataset big enough? Sample size requirements when using artificial neural networks for discrete choice analysis. J. Choice Modell. 28, 167–182. <https://doi.org/10.1016/j.jocm.2018.07.002>.
- Alwosheel, Ahmad, Van Cranenburgh, Sander, Chorus, Caspar, 2019. 'Computer says no' is not enough: Using prototypical examples to diagnose artificial neural networks for discrete choice analysis. Journal of Choice Modelling 33.
- Ancona, M., Ceolini, E., Öztireli, C., Gross, M., 2017. A unified view of gradient-based attribution methods for deep neural networks. Explaining and Visualizing Deep Learning.
- Bach, S., Binder, A., Montavon, G., Klauschen, F., Müller, K.-R., Samek, W., 2015. On pixel-wise explanations for non-linear classifier decisions by layer-wise relevance propagation. PLoS ONE 10 (7), e0130140.
- Batista, G.E., Prati, R.C., Monard, M.C., 2004. A study of the behavior of several methods for balancing machine learning training data. ACM SIGKDD Explorations Newsletter 6 (1), 20–29.
- Bishop, C.M., 1995. Neural networks for pattern recognition. Oxford University Press.
- Bishop, C.M., 2006. Pattern recognition and machine learning. Springer.
- Böhle, M., Eitel, F., Weygandt, M., Ritter, K., 2019. Layer-wise relevance propagation for explaining deep neural network decisions in MRI-based Alzheimer's disease classification. Front. Aging Neurosci. 11, 194.
- Chawla, N.V., Bowyer, K.W., Hall, L.O., Kegelmeyer, W.P., 2002. SMOTE: synthetic minority over-sampling technique. J. Artificial Intell. Res. 16, 321–357.
- Chen, C., Ma, J., Susilo, Y., Liu, Y., Wang, M., 2016. The promises of big data and small data for travel behavior (aka human mobility) analysis. Transport. Res. C: Emerg. Technol. 68, 285–299.
- Chiang, W.-Y.K., Zhang, D., Zhou, L., 2006. Predicting and explaining patronage behavior toward web and traditional stores using neural networks: a comparative analysis with logistic regression. Decis. Support Syst. 41 (2), 514–531.
- Chollet, F. (2015). Keras.
- Cybenko, G., 1989. Approximation by superpositions of a sigmoidal function. Math. Control, Signals Syst. (MCSS) 2 (4), 303–314.
- Doshi-Velez, F., & Kim, B. (2017). Towards a rigorous science of interpretable machine learning. arXiv preprint arXiv:1702.08608.
- Golshani, N., Shabanpour, R., Mahmoudfard, S.M., Derrible, S., Mohammadian, A., 2018. Modeling travel mode and timing decisions: comparison of artificial neural networks and copula-based joint model. Travel Behav. Soc. 10, 21–32.
- Goodfellow, I., Bengio, Y., Courville, A., 2016. Deep learning, (Vol. 1): MIT press Cambridge.
- Hagenauer, J., Helbich, M., 2017. A comparative study of machine learning classifiers for modeling travel mode choice. Expert Syst. Appl. 78, 273–282.
- Hall, P., Gill, N., 2018. An Introduction to Machine Learning Interpretability-Dataiku Version. O'Reilly Media, Incorporated.
- Haykin, S.S., 2009. Neural networks and learning machines, (Vol. 3): Pearson Upper Saddle River.
- He, H., Garcia, E.A., 2008. Learning from imbalanced data. IEEE Transactions on Knowledge & Data Engineering(9), 1263–1284.
- Hensher, D.A., Ton, T.T., 2000. A comparison of the predictive potential of artificial neural networks and nested logit models for commuter mode choice. Transport. Res. E: Logist. Transport. Rev. 36 (3), 155–172.
- Hillel, T., Elshafie, M., Ying, J., 2018. Recreating passenger mode choice-sets for transport simulation: A case study of London, UK. Proceedings of the Institution of Civil Engineers - Smart Infrastructure and Construction, 171(1), 29–42. doi:10.1680/jsmic.17.00018.
- Hillel, T., Elshafie, M.Z., Jin, Y., 2018b. Recreating Passenger Mode Choice-Sets for Transport Simulation. In: Proceedings of the Institution of Civil Engineers-Smart Infrastructure and Construction, pp. 1–49.
- Hornik, K., Stinchcombe, M., White, H., 1989. Multilayer feedforward networks are universal approximators. Neural Networks 2 (5), 359–366.
- Karlaftis, M.G., Vlahogianni, E.I., 2011. Statistical methods versus neural networks in transportation research: differences, similarities and some insights. Transport. Res. C: Emerg. Technol. 19 (3), 387–399.
- Kingma, D.P., Ba, J., 2014. Adam: A method for stochastic optimization. arXiv preprint arXiv:1412.6980.
- Kittley-Davies, J., Alqaraawi, A., Yang, R., Costanza, E., Rogers, A., Stein, S., 2019. Evaluating the effect of feedback from different computer vision processing stages: a comparative lab study. Paper presented at the Proceedings of the 2019 CHI Conference on Human Factors in Computing Systems.
- Krizhevsky, A., Sutskever, I., Hinton, G.E., 2012. Imagenet classification with deep convolutional neural networks. Paper presented at the Advances in neural information processing systems.
- Lapuschkin, S., Binder, A., Montavon, G., Müller, K.-R., Samek, W., 2016a. Analyzing classifiers: Fisher vectors and deep neural networks. Paper presented at the Proceedings of the IEEE Conference on Computer Vision and Pattern Recognition.
- Lapuschkin, S., Binder, A., Montavon, G., Müller, K.-R., Samek, W., 2016b. The LRP toolbox for artificial neural networks. J. Mach. Learn. Res. 17 (1), 3938–3942.
- LeCun, Y., Bengio, Y., Hinton, G., 2015. Deep learning. Nature 521 (7553), 436–444.
- LeCun, Y.A., Bottou, L., Orr, G.B., Müller, K.-R., 2012. Efficient backprop Neural networks: Tricks of the trade (pp. 9–48): Springer.
- Lee, D., Derrible, S., Pereira, F.C., 2018. Comparison of four types of artificial neural network and a multinomial logit model for travel mode choice modeling. Transp. Res. Rec. 2672 (49), 101–112.
- Lipton, Z. C. (2016). The mythos of model interpretability. arXiv preprint arXiv:1606.03490.
- Ma, X., Dai, Z., He, Z., Ma, J., Wang, Y., Wang, Y., 2017. Learning traffic as images: a deep convolutional neural network for large-scale transportation network speed prediction. Sensors 17 (4), 818.
- Mckinney, S.M., Sieniek, M., Gilbert, F., Godbole, V., Godwin, J., Antropova, N., Corrado, G.C., 2020. International evaluation of an AI system for breast cancer screening. Nature 577, 89–94. <https://doi.org/10.1038/s41586-019-1799-6>.
- Montavon, G., Samek, W., Müller, K.-R., 2018. Methods for interpreting and understanding deep neural networks. Digital Signal Process. 73, 1–15.
- Olah, C., Satyanarayan, A., Johnson, L., Carter, S., Schubert, L., Ye, K., Mordvintsev, A., 2018. The building blocks of interpretability. Distill, 3(3), e10.
- Polson, N.G., Sokolov, V.O., 2017. Deep learning for short-term traffic flow prediction. Transport. Res. C: Emerg. Technol. 79, 1–17.
- Ribeiro, M.T., Singh, S., Guestrin, C., 2016. Why should I trust you?: Explaining the predictions of any classifier. Paper presented at the Proceedings of the 22nd ACM SIGKDD international conference on knowledge discovery and data mining.
- Rosenfeld, A., Richardson, A., 2019. Explainability in human-agent systems. Auton. Agent. Multi-Agent Syst. 1–33.

- Samek, W., Binder, A., Montavon, G., Lapuschkin, S., Müller, K.-R., 2016. Evaluating the visualization of what a deep neural network has learned. *IEEE Trans. Neural Networks Learn. Syst.* 28 (11), 2660–2673.
- Samek, W., Montavon, G., Vedaldi, A., Hansen, L.K., Müller, K.-R., 2019. *Explainable AI: Interpreting, Springer Nature, Explaining and Visualizing Deep Learning.*
- Samek, W., Wiegand, T., Müller, K.-R., 2017. Explainable artificial intelligence: Understanding, visualizing and interpreting deep learning models. arXiv preprint arXiv:1708.08296.
- Shrikumar, A., Greenside, P., Kundaje, A., 2017. Learning important features through propagating activation differences. Paper presented at the Proceedings of the 34th International Conference on Machine Learning-Volume 70.
- Simonyan, K., Vedaldi, A., & Zisserman, A. (2013). Deep inside convolutional networks: Visualising image classification models and saliency maps. arXiv preprint arXiv:1312.6034.
- Springenberg, J. T., Dosovitskiy, A., Brox, T., Riedmiller, M., 2014. Striving for simplicity: The all convolutional net. arXiv preprint arXiv:1412.6806.
- Sturm, I., Lapuschkin, S., Samek, W., & Müller, K.-R. (2016). Interpretable deep neural networks for single-trial EEG classification. *Journal of neuroscience methods*, 274, 141–145. Retrieved from https://ac.els-cdn.com/S0165027016302333/1-s2.0-S0165027016302333-main.pdf?_tid=4c0bab3e-6118-46f8-bf06-3493003c3030&acdnat=1543322943_6f905b08777843ee3531cb62f98ddd56.
- Sun, Y., Jiang, Z., Gu, J., Zhou, M., Li, Y., Zhang, L., 2018. Analyzing high speed rail passengers' train choices based on new online booking data in China. *Transport. Res. C: Emerg. Technol.* 97, 96–113.
- Xie, D.-F., Fang, Z.-Z., Jia, B., He, Z., 2019. A data-driven lane-changing model based on deep learning. *Transport. Res. C: Emerg. Technol.* 106, 41–60.
- Yao, H., Wu, F., Ke, J., Tang, X., Jia, Y., Lu, S., . . . Li, Z., 2018. Deep multi-view spatial-temporal network for taxi demand prediction. Paper presented at the Thirty-Second AAAI Conference on Artificial Intelligence.
- Zeiler, M.D., Fergus, R., 2013. Stochastic pooling for regularization of deep convolutional neural networks. arXiv preprint arXiv:1301.3557.
- Zintgraf, L.M., Cohen, T.S., Adel, T., Welling, M., 2017. Visualizing deep neural network decisions: Prediction difference analysis. arXiv preprint arXiv:1702.04595.
- Van Cranenburgh, S., Wang, S., Vij, A., Pereira, F., Walker, J., 2021. Choice modelling in the age of machine learning. arXiv preprint arXiv:2101.11948.
- Van Cranenburgh, S., Kouwenhoven, M., 2020. An artificial neural network based method to uncover the value-of-travel-time distribution. *Transportation*.